J Electroceram (2008) 20:3–9
DOI 10.1007/s10832-007-9329-6

Numerical modelling of ceramic mems structures with piezoceramic thick films

Marina Santo Zarnik · Darko Belavic · Hana Ursic · Srecko Macek

Received: 9 March 2007 / Accepted: 4 September 2007 / Published online: 25 September 2007

Abstract The correctness of the material parameters that are used in numerical models is of key importance for any numerical analysis. Because of a lack of available material parameters and standard procedures for characterising piezoceramic thick films, special attention has to be paid to providing data for accurate material models. In the presented work, thick-film (TF) lead–zirconate–titanate (PZT) structures made on different ceramic substrates were considered. In order to obtain proper material parameters for TF PZT some unconventional characterisation approaches were used e.g. nano-indentation test for evaluation of the compliance of the piezo film. The results of characterising TF PZT structures on two different ceramic substrates, Al_2O_3 and pre-fired low temperature cofired ceramic (LTCC), are presented. For validation purposes simple cantilever-type actuators were modelled using the piezoelectric coupled-field capabilities of the finite-element (FE) package Ansys/Multiphysics and simulation results were compared with the measurements of the real structures.

Keywords Thick-film PZT · Nanoindentation · Finite-element analysis · LTCC · d_{31}

1 Introduction

Finite-element analyses (FEAs) are widely used in the research and initial design phases of various MEMS devices as well as for optimising the final products. However, analysts should be aware that use of theoretical material properties can result in an unacceptable discrepancy between the predictions and the real device properties. This is one of the main problems with modelling of sensor and actuator structures with thick piezoceramic films. The effective material properties of the piezoceramic thick film depend not only on the material composition but also on the compatibility of the film with the other materials e.g. the thick-film electrodes and the ceramic substrate, and the processing conditions [2–9]. In order to obtain accurate material parameters for a certain thick-film piezoelectric structure, extensive experimental work is required.

In this study we describe an experimental procedure used for characterising PZT ($Pb(Zr_{0.53},Ti_{0.47})O_3$) thick films processed on two different ceramic substrates: Al_2O_3 and pre-fired LTCC. The elastic properties of the TF PZT were obtained from nano-indentation tests. The effective transverse piezoelectric coefficient $e_{31,f}$ was evaluated from the results of substrate-flexure measurements by taking into account the thickness of the PZT film as was previously described in [9]. These experimentally evaluated material parameters were then used in FE models of simple actuator structures, which were built using the piezoelectric coupled-field capability of the ANSYS/Multiphysics software. For validation purposes appropriate test actuators were prepared and measured. The results were compared to the results of the simulations and were used to assess the validity of the models and the proposed characterisation procedure.

2 Finite-element modelling

In piezoelectric materials, elastic and electric fields are coupled so that the physics of both fields needs to be solved simultaneously. Mechanical stress $\{T\}$ and strain $\{S\}$ are

M. S. Zarnik · D. Belavic
HIPOT–R&D,
Trubarjeva 7,
8310 Šentjernej, Slovenia

M. S. Zarnik (✉) · D. Belavic · H. Ursic · S. Macek
Jožef Stefan Institute,
Jamova 39,
1000 Ljubljana, Slovenia
e-mail: marina.santo@ijs.si

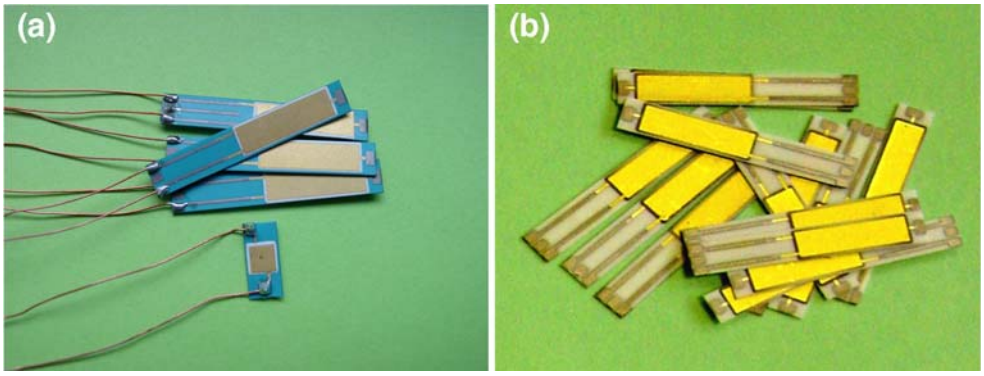

Fig. 1 Test samples on the LTCC substrates (**a**) and Al_2O_3 substrates (**b**) used for characterisation of the PZT film and validation of the FE model

related to dielectric displacement $\{D\}$ and electric field $\{E\}$ as stated in the following constitutive equations:

$$\begin{aligned}\{\mathrm{S}\} &= [s^{\mathrm{E}}]\{T\} + [d]\{E\} \\ \{D\} &= [d]^{\mathrm{T}}\{T\} + [\varepsilon^T]\{E\}\end{aligned} \tag{1}$$

where $[s^E]$ is the compliance matrix evaluated at constant electric field, $[\varepsilon^T]$ is the permittivity matrix evaluated at constant stress and $[d]$ is the piezoelectric matrix relating strain to electric field. The above relationship provides a basis for the FEA piezoelectric matrix equations:

$$\begin{bmatrix} M & 0 \\ 0 & 0 \end{bmatrix} \begin{Bmatrix} \ddot{u} \\ \ddot{V} \end{Bmatrix} + \begin{bmatrix} C^u & 0 \\ 0 & C^V \end{bmatrix} \begin{Bmatrix} \dot{u} \\ \dot{V} \end{Bmatrix} + \begin{bmatrix} K^u & K^Z \\ K^{Z^T} & K^V \end{bmatrix} \begin{Bmatrix} u \\ V \end{Bmatrix} = \begin{Bmatrix} F \\ L \end{Bmatrix} \tag{2}$$

In Eq. 2 $[M]$ represents the structural mass calculated from the material density, $[C^u]$ is the structural damping matrix, $[C^V]$ represents dielectric losses, matrix $[K^Z]$ contains piezoelectric coefficients in $[d]$ form (strain/electric field) or $[e]$ form (stress/electric field), $[K^u]$ contains elastic properties of the piezo material, which can be input as compliance $[s^E]$ or stiffness $[c^E]$ coefficients and $[K^V]$ is the permittivity matrix with permittivity values evaluated at constant strain $[\varepsilon^s]$ or constant stress $[\varepsilon^T]$ and $\{u\}$ and $\{V\}$ are displacement electrical potential vectors. $\{F\}$ and $\{L\}$ denote the structural and electrical loads respectively. Superscript T denotes a transpose of the matrix.

3 Test samples

The PZT thick films were made by screen printing the PZT 53/47 paste made at the Jožef Stefan Institute [6, 7], pre-firing at 450°C for 60 min and firing for 60 min in a belt furnace at a peak temperature of 850°C. They were poled with an electrical field of 75 kV/cm perpendicular to the film plane in a silicon–oil bath at 100°C, for 20 min.

Test samples used for characterisation of the PZT film and validation of the FE model are presented in Fig. 1. The length of the substrates is 25 mm, the length of the TF PZT patch with thick-film Au electrodes on the top and bottom is 12 mm, the thickness of the LTCC substrates is 200 μm, the thickness of the Al_2O_3 substrates is 250 μm, the thickness of the PZT film is 42±3 μm and the thickness of the electrodes is 3 μm. The film thickness was obtained from measurements of the surface profile of several samples at different positions.

4 Characterisation of the PZT thick film

The compliance parameters of the PZT thick film were obtained from the measurements of the indentation modulus that were conducted using a Fisherscope H100C nano-indenter system as described in [9]. Even though such a test is not common for measuring the elasticity of an anisotropic

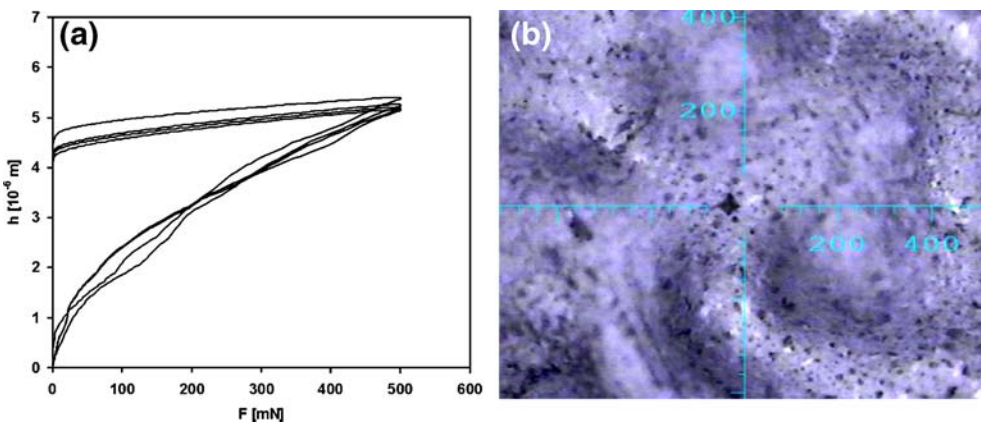

Fig. 2 (**a**) Measured indentation curves for the 50-μm thick PZT film on Al_2O_3, (**b**) Residual plastic indentation in the PZT film

Table 1 Compliance components for TF PZT on Al_2O_3 and LTCC substrates calculated with experimentally obtained Young's moduli Y_{it33} and the assumed Poisson's ratio.

Parameter	TF PZT/Al_2O_3 (m^2/N)	TF PZT/LTCC (m^2/N)
s^E_{11}	3.39×10^{-11}	6.14×10^{-11}
s^E_{33}	4.21×10^{-11}	7.61×10^{-11}
S^E_{12}	-1.00×10^{-11}	-1.81×10^{-11}
S^E_{13}	-1.43×10^{-11}	-2.58×10^{-11}
S^E_{44}	1.19×10^{-10}	2.14×10^{-10}
S^E_{66}	9.45×10^{-11}	1.71×10^{-10}

material, the big advantage of the technique is that it is a local measurement and only small volumes of the material are needed. Even neglecting the effect of the internal stresses on the material properties during the measurement, which may result in less accurate results, this technique could still be appropriate for the characterisation of piezoceramic films. This technique enables us to asses at least some information about the film elastic properties. The most important requirement is that the film must be thick enough to avoid the influence of the substrate. The result of the nano-indentation measurement is the indentation modulus (Y_{it}) which is comparable to the Young's modulus of the tested material. Y_{it} is determined according to the European standard [10] by:

$$Y_{it} = \frac{1-\nu^2}{\frac{1}{Y_r} - \frac{1-\nu_i^2}{Y_i}} \tag{3}$$

where ν and ν_i are the Poisson's ratios of the tested material and the indenter, Y_i is the Young's modulus of the indenter (for diamond Y_i=1,140 GPa and ν_i=0.07) and Y_r is a reduced modulus of the indentation contact. Y_r is calculated from the compliance of the contact at the maximum test force (dh/dF) and the projected contact area.

As an example, the indentation curves obtained from measuring a thick-film PZT on an Al_2O_3 sample and the aspect of the residual plastic indentation are presented in Fig. 2.

The indenter was pushed into the PZT film in the poling direction, so that the Young's modulus Y_{33} was obtained from these measurements. In order to avoid the influence of the top electrode, it was carefully removed after poling. Since there was not any electrical load used during the measurements, we presumed that the measured Y_{33} corresponds to C^D_{33}. For the rough estimation we assumed the thick PZT film has the same Poison's ratio as the bulk material (PZT 52/48 [1] was used as a reference) and the same ratio between the C^D_{ij} components. This way all the stiffness components can be calculated from only one measured indentation modulus. By transforming the C^D_{ij} components to S^D_{ij} and then using the same ratio between the parameters S^D_{ij} and S^E_{ij} as reported for bulk PZT 52/48 in [1] the compliance parameters S^E_{ij} of the PZT film were calculated. Although not of high accuracy (due to the above assumptions), we presumed that these results are good enough to be used in the numerical analysis aimed at revealing the trends.

The average indentation modulus Y_{it33} measured on several samples was 47 GPa±10% for TF PZT/Al_2O_3 and 22 GPa±11% for TF PZT/LTCC. From these values Young's modulus of 54 and 30 GPa were calculated, which are comparable to the values reported for soft PZT and hard PZT thick films in [5]. The resulting compliance components for TF PZT on Al_2O_3 and LTCC substrates are collected in Table 1.

The effective piezoelectric transverse coefficient, $e_{31,f}$, of the thick-film PZT poled perpendicular to the film plane, was evaluated based on the method published for the thin piezoelectric films, [2], as described in [9]. The measure-

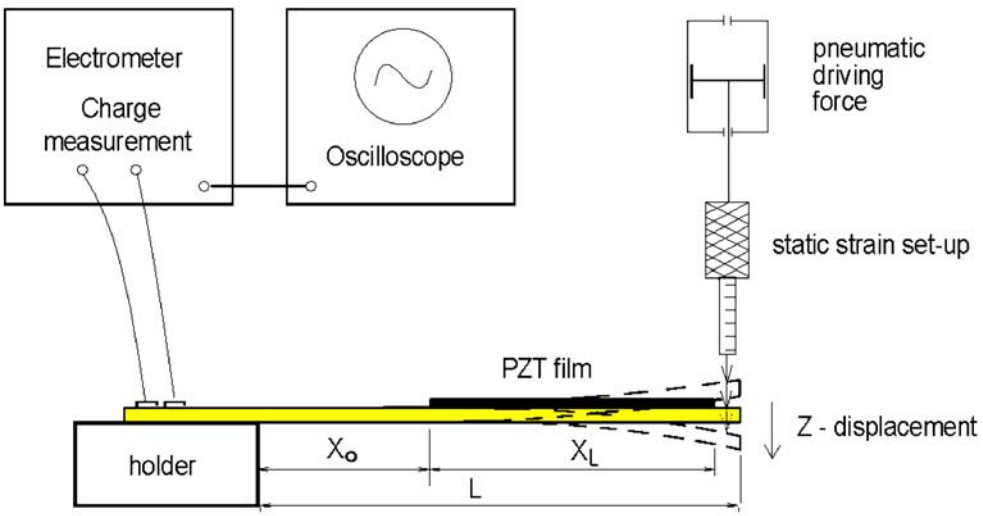

Fig. 3 Schematic representation of the experimental set-up for the measurement of $e_{31,f}$

Table 2 Experimentally obtained transverse and direct piezoelectric coefficients for TF PZT on two different substrates.

Structure	$e_{31,f}$ [C/m^2]	$D_{31,f}$ (pC/N)	$d_{33,f}$ (pC/N)
TF PZT/Al_2O_3	1.21	28.9	125±5%
TF PZT/LTCC	0.16	8.5	40±5%

ment set-up with pneumatically controlled forced deflection of the cantilever is presented in Fig. 3.

In order to derive the charge built up on the piezoceramic thick film, the flux D across the area of the top electrode can be evaluated by integrating over the electrode surface. For a rectangular electrode with a constant width this is expressed by:

$$Q = w\int_{x_0}^{x_l} D_3 dx \tag{4}$$

where Q is the charge, w is the width of the electrode, and the length of the electrode is equal to $x_1 - x_0$.

Considering in Eq. 1 the conditions set by the measurement procedure i.e., the electrical charge generated between the electrodes in sensor mode is measured at zero electrical field, and the TF PZT is free to move in the z-direction, so that the stress component in this direction is assumed to be zero, the dielectric displacement on the plane of the substrate's surface can be expressed by:

$$D_3 = \frac{d_{31}}{s_{11}^E + s_{12}^E} \cdot (S_1 + S_2) = e_{31.f} \cdot (S_1 + S_2) \tag{5}$$

where $e_{31,f}$ is the effective piezoelectric coefficient and S_1 and S_2 are transverse strain components.

Taking into the account the thickness of the PZT film and neglecting the difference between the Poisson's ratios of the substrate and the film, the dielectric displacement on the top surface of the PZT film can be expressed by introducing the linear proportion factor k:

$$\begin{aligned} D_{3\,top} &= e_{31.f} \cdot (1 - \nu_s) \cdot \left(1 + 2\frac{h_p}{h_s}\right) \cdot S_1 \\ &= e_{31.f} \cdot (1 - \nu_s) \cdot k_t \cdot S_1 \end{aligned} \tag{6}$$

Table 3 Young's moduli and densities used in the FE model.

Material	Y (Gpa)	ν (–)	ρ (kg m^{-3})
TF PZT	Table 1	Table 1	7,700
Al_2O_3	340	0.23	3,780
LTCC	110	0.17	3,100
Au electrode	83	0.43	19,300

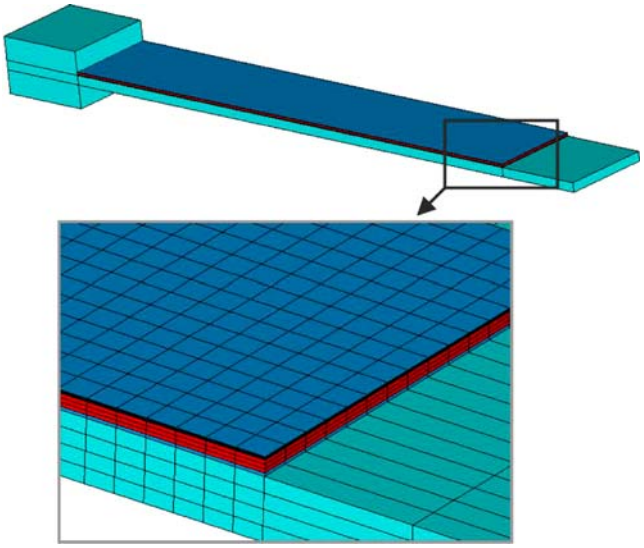

Fig. 4 Geometrical model: half symmetry of the actuator with a meshed detail

where h_p is the thickness of the film, h_s is the thickness of the substrate, ν_s is the Poisson's coefficient of the substrate material and the factor $k_t = 1 + 2h_p/h_s$.

Taking in Eq. 6 an average strain S_1, calculated in the plane of half of the thickness of the PZT film ($z = h_p/2$) the effective piezoelectric transverse coefficient can be derived from the following equation:

$$e_{31,f} = \frac{2l^3 Q}{3k \cdot whz_l(1 - \nu_s) \cdot \left(l(x_l - x_0) - \left(x_l^2 - x_0^2\right)/2\right)} \tag{7}$$

where l, w and h are the length, width and thickness of the bending part of the substrate, the length of the top electrode is $L_x = (x_1 - x_0)$ and z_l is the tip displacement.

The $d_{31,f}$ coefficients were then calculated from the equation:

$$d_{31,f} = e_{31,f} \cdot \left(s_{11}^E + s_{12}^E\right) \tag{8}$$

in which s parameters according to Table 1 were used.

The direct piezoelectric coefficients were evaluated by using different characterization techniques: laser interferometery, PFM and the Berlincourt method [12]. Since d_{33} has a negligible effect on the bending properties of the transversal mode actuator, the evaluated values for $d_{33,f}$ are here considered only as supplementary information about

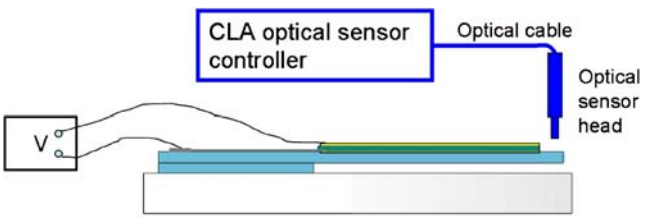

Fig. 5 Schematic representation of the experimental set-up

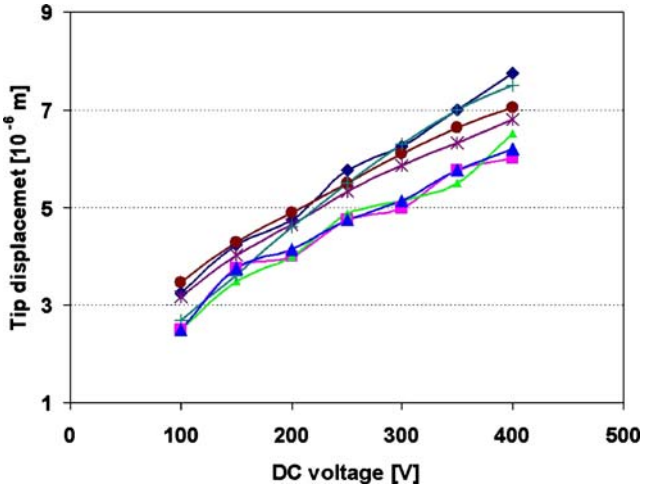

Fig. 6 Tip-displacement versus applied voltage characteristics measured for seven test samples of the TF PZT cantilever-type actuator made on Al_2O_3

the treated PZT thick films. All the measured piezoelectric coefficients are collected in Table 2.

The relative dielectric constant measured in the poling directions at 1 kHz was 490 for TF PZT/Al_2O_3 and 200 for TF PZT/LTCC. The dielectric loss tangents measured at the same conditions were 0.020 and 0.016 for TP PZT on Al_2O_3 and LTCC respectively.

5 Model validation

The material parameters specified in Tables 1, 2 and 3 were used as material inputs in the FE models of the simple cantilever structure presented in Fig. 4. The length of the cantilever is 14 mm, the length and thickness of the PZT patch are 12 mm and 40 μm respectively, and all the other geometrical details used were according to the real test samples presented in Fig. 1. The models of the geometrical

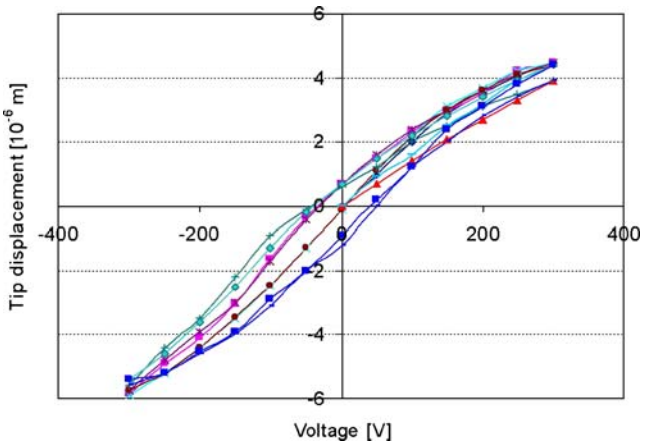

Fig. 7 Tip-displacement versus applied voltage characteristics measured for four test samples of the TF PZT cantilever-type actuator made on LTCC

Table 4 Displacement of the tip of the actuators (at L=13.5 mm), at the electrical load of 200 V dc applied between the electrodes.

Actuator structure	Simulated displacement (μm)	Measured displacement[a] (μm)
TF PZT/Al_2O_3	4.4	4.35±0.5
TF PZT/LTCC	3.0	3.05±0.3

[a] The average value extracted from the virgin curves

structures are meshed with coupled-field solid elements Solid 5 and 226 with the structural and electric degree of freedom (*df*). The elements support nonlinear static, modal, harmonic response and transient analyses. In the present case study we performed only static and harmonic analyses. The Young's moduli and densities used in the model are collected in Table 3. The densities for Al_2O_3 and LTCC were obtained from the producer data sheets. The density of the PZT film was estimated as an average value of the several reported densities from the literature. For the Au electrodes, the density of bulk Au was used (http://www.efunda.com). Young's modulus of elasticity of LTCC was obtained from flexural tests performed in a universal testing-machine, Instron 4301, using a three-point bending fixture according to the ASTM Standard C 1161-90. The accuracy of this result is ±10%. Flexural tests performed on non-standard 250-μm thick Al_2O_3 test patterns showed mean a value of 340 GPa±10%, which is in good agreement with the Young's modulus declared by the producer.

Validation of the FE model was performed in two steps. In the first step, the bending behaviour of the actuator was considered at dc electrical load. The measurement of the actuator's tip displacements was conducted with an experimental set-up that uses a high-resolution optical sensor based on confocal chromatic technology. The test actuators were prepared by attaching the test samples (Fig. 1) to the fixed ceramic carriers to form cantilever structures in such a

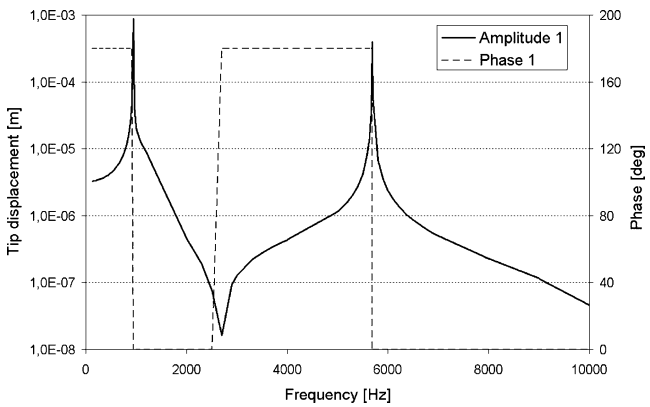

Fig. 8 Results of the harmonic analysis of the TF PZT/LTCC cantilever-type actuator

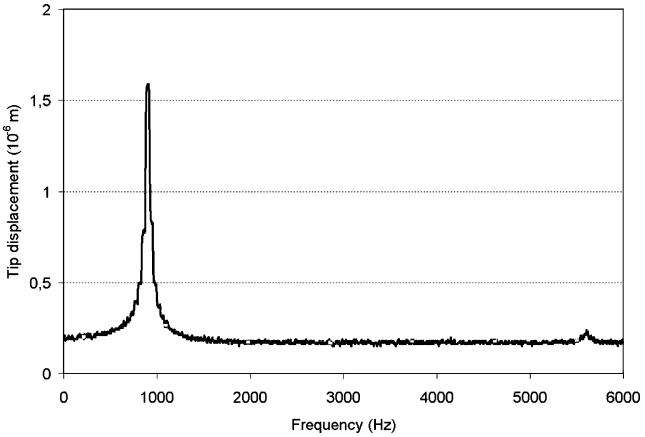

Fig. 9 Measured resonance frequency of the TF PZT/LTCC test actuator

way that the edge of the thick-film PZT patches was placed just near to the fixation point of the cantilever. In this way the length of the cantilever was 14 mm, while the length of the active PZT film and electrodes was 12 mm. The measurements of the tip displacement were performed at L=13.5 mm from the fixation point. The schematic representation of the measurement set-up is represented in Fig. 5. The resolution of the chromatic length aberration (CLA) sensor is 10 nm, while the accuracy of the whole experimental set-up is estimated to be 100 nm.

The results obtained from measuring several test actuators on Al_2O_3 and LTCC substrates are presented in Figs. 6 and 7 respectively. In order to avoid the position errors resulting from a non negligible amount of creep, in the case of the actuators on Al2O3 substrates, only details of the virgin curves (Fig. 6) were used for validation purposes. The FEA results that were obtained using the material parameters according to Tables 1, 2 and 3, and for an electric load of 200 V dc, showed for the actuator on an Al_2O_3 substrate a maximum deflection of 4.5 μm and for the actuator on a LTCC substrate a maximum deflection of 3 μm. Notice that the FE model was built assuming linear material behaviours and that the hysteresis inherent to the piezoceramic materials was neglected. Also, an ideal clamping of the cantilever was assumed neglecting the strains in the adhesive material. Taking this into account the numerical and experimental results were in relatively good agreement as evident from Table 4.

In the second step the harmonic behaviours of the test actuators were considered. Because of a lack of experimental data for the density of TF PZT, the harmonic analysis was performed using an assumed density of 7,700 kg/m^3. Since the thickness of the substrate is five times higher than the thickness of the PZT film, and there is also some influence of the dense Au electrodes, we presumed that using such an estimated value in the harmonic analyses can still be acceptable to show the trends. The main aim of this step of the validation procedure was only to check the fundamental (first natural resonance frequency) and first overtone resonance frequency of the vibrating cantilever. Besides, from the impedance measurements the resonance frequencies were assessed by using an MTI-2100 Fotonic sensor with a high resolution probe module. The simulation results and the measured tip-displacement versus frequency characteristics of the test actuator made on LTCC substrate are presented in Figs. 8 and 9 respectively. The FEA results as well as analytical calculations (using the expressions from [11]) were close to the measured fundamental resonance frequency of 914 Hz (Table 5).

Table 5 Calculated and experimental resonance frequencies.

Vibration mode	Analytical f_{res} (Hz)	FEA f_{res} (Hz)	Measured f_{res} (Hz)
Fundamental	909	918	914
First overtone	5,730	5,688	5,620

6 Conclusions

In order to obtain accurate material models for TF PZT on different ceramic substrates, unconventional characterisation techniques were used such as a nano-indentation test for evaluation of the material compliance, and a substrate-flexural method for evaluation of the d_{31} coefficient. Results of the FE analysis obtained from using the experimentally obtained material parameters were in good agreement with the experimental results. This confirmed the adequacy of the characterisation procedure and validated the material models for TF PZT on Al_2O_3 and LTCC substrates. These can be now used with more confidence for numerical modelling of more complex MEMS structures.

Acknowledgement Part of this work is supported by the EC through the NoE MIND (FP6, contract no. NMP2-CT-2004-505657) and the MINUET project (FP6, contract no. NMP3-CT-2005-515757) and by the Slovenian Research Agency in the frame of the project L2-9583. The authors would like to thank Mr. Mitja Jerlah, HIPOT–R&D for manufacturing the thick-film test samples and the staff of the Electronic Ceramics department from the Joef Stefan Institute for preparing the PZT paste and for helpful discussions.

References

1. B. Jaffe, W.R. Cook, H. Jaffe, *Piezoelectric ceramics*. (Academic, London, 1971)
2. M. A. Dubois, P. Muralt, Measurement of effective transverse piezoelectric coefficient e31,f of AIN and Pb(Zrx, Ti1-x)O3 thin films, Sens. Actuators, A **77**, 106 (1999)
3. I. Kanno, H. Kotera, K. Wasa, Measurement of transverse piezoelectric properties of PZT thin films, Sens. Actuators, A **107**, 68 (2003)

4. R.N. Torah, S.P. Beeby, N.M. White, Experimental investigation into the effect of substrate clamping on the piezoelectric behaviour of thick-film PZT elements, J. Phys. D: Appl. Phys. **37**, 1 (2004)
5. V. Walter, P. Delobelle, P. Le Moal, E. Joseph, M. Collet, A piezo-mechanical characterisation of PZT thick films screen-printed on alumina substrate, Sens. Actuators, A **96**, 157 (2002)
6. M. Hrovat, J. Holc, S. Drnovšek, D. Belavič, J. Bernard, M. Kosec, L. Golonka, A. Dziedzic, J. Kita, Characterisation of PZT thick films fired on LTCC substrates, J. Mater. Sci. Lett. **22**(17), 1193 (2003)
7. L. Golonka, M. Buczek, M. Hrovat, D. Belavič, A. Dziedzic, H. Roguszczak, T. Zawada, Properties of PZT thick films made on LTCC, Microelectron. Int. **22**(2), 13 (2005)
8. D. Damjanovic, Ferroelectric, dielectric and piezoelectric properties of ferroelectric thin films and ceramics, Rep. Prog. Phys. **61**, 1276 (1998)
9. M. S. Zarnik, D. Belavic, S. Macek, Evaluation of the constitutive material parameters for the numerical modelling of structures with lead–zirconate–titanate thick films, Sens. Actuators, A **136**(2), 618 (2007)
10. European standard EN ISO 14577-1, Metallic materials—instrumented indentation test for hardness and materials parameters—part 1: Test method, (2002)
11. Qing-Ming Wang, et al., Nonlinear piezoelectric behaviour of ceramic bending mode actuators under strong electric fields, J. Appl. Phys. **86**(6), 3352 (1999)
12. H Uršič, M. Hrovat, B. Malič, M. Kosec, Piezoelectric measurements of thick an thin PZT films on different substrates (IJS report, 9495, 2006)
13. 951 low-temperature cofire dielectric tape, DuPont Photopolymer & Electronic Materials, L-11590